Research Square

Preprints are preliminary reports that have not undergone peer review.
They should not be considered conclusive, used to inform clinical practice,
or referenced by the media as validated information.

Identification of the type II NAD(P)H dehydrogenase gene family reveals that TaNDC1 positively regulate Fusarium head blight resistance in wheat

Puwen Song
Henan Institute of Science and Technology
Liuliu Wu
Xinyang Agriculture and Forestry University
Ao Li
Henan Institute of Science and Technology
Dan Li
Henan Institute of Science and Technology
Yiyao Li
Henan Institute of Science and Technology
Ping Hu
Henan Institute of Science and Technology
Yuanyuan Guan
Henan Institute of Science and Technology
Meng Zhang
Henan Institute of Science and Technology
Qili Liu
Henan Institute of Science and Technology
Haiyan Hu
haiyanhu@hist.edu.cn
Henan Institute of Science and Technology
Zhengang Ru
Henan Institute of Science and Technology

Research Article

Keywords: TaNDs, TaNDC1, Fusarium head blight, wheat, genome-wide, expression, hormone, stress

Posted Date: July 13th, 2026

DOI: https://doi.org/10.21203/rs.3.rs-9811731/v1

License: This work is licensed under a Creative Commons Attribution 4.0 International License.
Read Full License

Additional Declarations: No competing interests reported.

Abstract

Background

The type II NAD(P)H dehydrogenase (*ND*) gene family, as key components of the non-phosphorylating alternative respiratory pathway in mitochondria, plays important roles in plant responses to various environmental stresses. The *ND* gene family has been well characterized in multiple species, yet comprehensive studies on this gene family in wheat remain unexplored.

Results

The study identified 16 *ND* genes, and evolutionary and syntenic analyses revealed that all three subfamilies of plant *ND* genes, *NDA*, *NDB* and *NDC* are present in wheat. Chromosomal distribution analysis demonstrated that *TaNDAs* and *TaNDBs* have homologs across all three subgenomes (A, B, and D), while *TaNDC1* exists as a single copy exclusively on chromosome 7D. *TaND* genes within the same phylogenetic group exhibited similar gene structures and conserved motif distributions. Promoter analysis showed that *TaNDs* widely harbored *cis*-acting elements associated with hormone signaling, stress responses, growth and development. Expression profiling demonstrated that *TaNDs* exhibited strong response to hormones, biotic and abiotic stresses. It is noteworthy that under infections of powdery mildew and crown rot, the expression of *TaNDC1* was suppressed, exhibiting a trend similar to that observed under SA treatment. Conversely, under Fusarium head blight (FHB) infection, its expression was strongly induced, mirroring the pattern seen under JA treatment. Functional studies demonstrated that silencing *TaNDC1* reduced wheat resistance to FHB, confirming its positive regulatory role in FHB resistance. Additionally, we confirmed that TaNDC1 interacts with TaPFT, a protein encoded within the major FHB resistance locus *Fhb1*.

Conclusions

This study enhance our understanding of the *TaND* gene family and identify *TaNDC1* as a potential candidate gene for improving FHB resistance in wheat.

Introduction

Mitochondria, as crucial sites for energy production in plants, not only possess the classical electron transport pathway coupled with ATP synthesis but also exhibit an alternative respiratory pathway composed of type II NAD(P)H dehydrogenases (NDs) and alternative oxidase (AOXs) [1]. This alternative pathway is involved in the thermogenesis of specific organs in some species and is thought to help prevent cell damage when exposed to environmental stress [2]. NDs are encoded by a small gene family and are categorized into three subgroups in plants: NDA, NDB, and NDC. NDA and NDC are localized on the inner surface of the mitochondrial inner membrane, whereas NDB is situated on the outer surface [3].

In *Arabidopsis thaliana*, seven *NDs* have been identified, comprising two members belong to the *NDA* family (*AtNDA1* and *AtNDA2*), four members belong to the *NDB* family (*AtNDB1* to *AtNDB4*), and one member belong to the *NDC* family (*AtNDC1*) [4–7]. It has been reported that these *NDs* are involved in responses to various environmental stresses. *AtNDA1* and *AtNDA2* play critical roles in plant responses to reoxygenation stress by safeguarding photosynthetic function and limiting reactive oxygen species (ROS) generation, thereby enhancing plant survival under hypoxia and reoxygenation conditions [8]. *AtNDB2* functions as the primary external NADH dehydrogenase in mitochondria, and in conjunction with *AtAOX1a* constitutes a complete, functional, non-phosphorylating electron transport pathway, whose operation enhances tolerance to drought and high light stress [6]. The transcriptome of knock-down of *AtNDB1* expression exhibits overlapping changes with those of the mutant lacking the *ABI4* transcription factor, suggesting that altered expression of *AtNDB1* can modulate plant defense signaling [9]. Altering the level of *AtNDB4* can induce changes in the expression of other alternative pathway genes, such as *AtNDB2* and *AtAOX1a*, and confers enhanced tolerance under salt stress [10]. *AtNDC1* regulates the biosynthesis of vitamin K1 in *Synechocystis* and *Arabidopsis* by performing the penultimate step [11]. NDs represent a class of redundant proteins with remarkable plasticity, enabling them to fulfill diverse roles in response to varying environmental conditions, thereby conferring organisms with enhanced adaptability.

Wheat (*Triticum aestivum* L.) belongs to the family *Poaceae* (*Gramineae*), *tribe Triticeae*, and genus *Triticum*. Since its evolutionary emergence and domestication approximately 10,000 years ago, it has gradually become the foremost global staple crop for human consumption, owing to its broad environmental adaptability and the protein-rich grains that are highly suitable for processing into a diverse array of food products. Hexaploid wheat (*Triticum aestivum* L.) harbors an expansive genome (~ 17 Gb) organized into three subgenomes (A, B, and D) that arose through two successive amphiploidization events [12]. The prevalence of repetitive sequences in the wheat genome has hindered comprehensive functional analyses of multigene families. During its growth and development, wheat is frequently subjected to infections by various pathogens, which can reduce grain yield and quality, thereby posing a significant threat to wheat production and global food security. Fusarium head blight (FHB), a worldwide disease caused by multiple species of Fusarium, manifests as seedling blight, stem base rot, stalk rot, and head blight [13]. Beyond reducing wheat yield, FHB-contaminated grains contain deoxynivalenol (DON), a mycotoxin produced by Fusarium species. DON poses severe risks to food safety and threatens the health of both humans and animals [14]. Although *NDs* are well-documented regulators of plant defense response to various environmental stresses, their specific roles in wheat remain poorly characterized. In this study, we systematically identify the *TaND* gene family in *Triticum aestivum* and characterize its members through phylogenetic, structural, and syntenic analyses. Expression profiling under hormonal, abiotic, and biotic stresses reveals distinct regulatory patterns. Functional assessment via VIGS demonstrates *TaNDC1*'s role in FHB resistance. This study provides foundational insights into *TaND* genes and highlights their potential as targets for wheat disease resistance breeding.

Materials and methods

Plant materials and stress treatments

The FHB-resistant wheat cultivar ‘Sumai 3’ was used in this study. Surface-sterilized seeds were germinated at 25°C in the dark and subsequently grown in a controlled environment chamber (16 h light/8 h dark, 25°C, 60% relative humidity) until the required developmental stages. For hormonal treatments, three-leaf-stage seedlings were sprayed with 100 μM methyl jasmonate (MeJA) or 5 mM salicylic acid (SA), with leaf samples collected at 0, 12, and 48 h post-treatment. For abiotic stress assays, seedlings were subjected to drought (20% PEG 6000) or heat stress (40°C), and samples were taken at 0, 6, and 10 h after stress initiation. For biotic stress evaluation, leaves of three-leaf-stage seedlings were inoculated with powdery mildew (*Blumeria graminis f. sp. tritici*) or Fusarium crown rot (*Fusarium spp.*), while for FHB challenge, spikes at anthesis were point-inoculated with 15 μL of a *Fusarium graminearum* (strain PH-1) spore suspension (5×10^5 spores mL^{-1}); tissues from all biotic assays were sampled at 0, 12, and 48 h post-inoculation. All collected samples were immediately frozen in liquid nitrogen and stored at − 80°C until RNA extraction. Primer sequences used in this study are listed in Supplementary Table S1.

Genome-wide identification and characterization of the TaND gene family

The Hidden Markov Model (HMM) profile of the NADH dehydrogenase domain (PF22366) was obtained from the Pfam database. A genome-wide search against the *Triticum aestivum* reference genome (IWGSC RefSeq v2.1) was performed using HMMER (E-value < 1×10^{-10}) [15]. Candidate proteins were verified for conserved ND domains using SMART tool (Schultz et al. 2000). The ExPASy ProtParam tool was used to predict basic physicochemical properties, including molecular weight, theoretical pI, and amino acid composition [17, 18].

Phylogenetic, gene structure, and conserved motif analyses

Full-length ND protein sequences from *Arabidopsis thaliana*, *Oryza sativa*, and *Triticum aestivum* were aligned using Clustal Omega (v1.2.4) [19]. Phylogenetic analysis was performed using MEGA11 software under the neighbor-joining method with 1000 bootstrap replicates [20]. Gene structures, including exon/intron organization, were predicted via the Conserved Domain Database (CDD) and visualized using TBtools software [21]. Conserved protein motifs were identified using the online MEME suite software with the maximum number of motifs set to 12, while all other parameters were maintained at default values [22]. The resulting motif architectures were graphically arranged using TBtools [23].

Chromosomal localization, gene duplication, and synteny analysis

Chromosomal positions of *TaND* genes were mapped based on the IWGSC genome annotation using MG2C v2.1 [24]. Intraspecific collinearity and gene duplication events were analyzed using the MCScanX algorithm of TBtools (Chen et al. 2020). Microsynteny analysis across wheat (*T. aestivum*), rice (*O. sativa*), maize (*Z. mays*), and Arabidopsis (*A. thaliana*) was performed using the Triticeae-GeneTribe (TGT) online platform [23].

Promoter cis-acting regulatory element analysis

The 2000-bp genomic sequences upstream of the translation start site of each *TaND* gene were extracted as putative promoter regions. *Cis*-acting regulatory elements were predicted using the PlantCARE database [25].

Expression profiling by quantitative RT-PCR (RT-qPCR)

Expression profiling by quantitative RT-PCR (RT-qPCR)
Total RNA was extracted from wheat tissues using the TRIzol method according to the manufacturer's instructions (TAKARA, Japan). First-strand cDNA was generated from total RNA with the PrimeScript RT Reagent Kit with gDNA Eraser (TAKARA, Japan). The relative expression of TaND genes was measured by RT-qPCR using ChamQ Universal SYBR qPCR Master Mix (Vazyme, Nanjing, China) on a QuantStudio 6 Flex Real Time PCR System (Applied Biosystems, USA). The TaActin gene served as the internal control in this experiment. The relative expression levels were calculated using the $2^{-\Delta\Delta Ct}$ method. The TBtools program was used to create the heatmap of the gene expression profile [23].

Yeast two-hybrid (Y2H) assay

The full-length coding sequences (CDS) of *TaNDC1*, *TaPFT* and *TaHRC* were cloned into the pGADT7 (AD) and pGBKT7 (BD) vectors, respectively. The resulting recombinant constructs were cotransformed into the yeast strain Y2HGold. Protein-protein interactions were assessed by monitoring yeast growth on synthetic defined (SD) medium lacking tryptophan and leucine (SD/-Trp-Leu), followed by selection on medium additionally lacking histidine and adenine with X-α-Gal (SD/-Trp-Leu-His-Ade- X-α-Gal). Appropriate controls were included, with pGBKT7-53/pGADT7-T serving as the positive control and empty vector combinations as negative controls.

Molecular docking simulations of the interaction between molecule TaPFT and molecule TaNDC1 were performed using AutoDock software, followed by visualization and analysis of the binding mode with PyMOL [26, 27].

Bimolecular fluorescence complementation (BiFC) assay

To validate protein-protein interactions in planta, the coding sequences (CDS) of *TaNDC1*, *TaPFT*, and *TaHRC* were used to generate BiFC constructs. *TaNDC1* was cloned into pEarleyGate201-cYFP (cYFP), while *TaPFT* and *TaHRC* were each independently cloned into pEarleyGate202-nYFP (nYFP), creating two test pairs: cYFP-TaNDC1/nYFP-TaPFT and cYFP-TaNDC1/nYFP-TaHRC. The recombinant plasmids were transformed into *Agrobacterium tumefaciens* strain GV3101. Bacterial cultures were co-infiltrated into leaves of *Nicotiana benthamiana* plants. After 48–72 h of incubation, reconstituted YFP fluorescence was observed using a laser-scanning confocal microscope.

Virus-induced gene silencing (VIGS) and FHB resistance assay

To silence *TaNDC1*, a 300-bp fragment from its 3'UTR region was amplified and inserted in reverse orientation into the γ-vector of barley stripe mosaic virus (BSMV), resulting in the construct BSMV:TaNDC1. In vitro-transcribed viral RNA was rub-inoculated onto flag leaves of wheat cultivar ‘Sumai 3’ at the booting stage, with BSMV:γ-inoculated plants used as the negative control. Silencing efficiency was verified by RT-qPCR 14 days post-inoculation. For the FHB resistance assay, silenced and control plants were challenge-inoculated at anthesis with a *Fusarium graminearum* (strain PH-1) spore suspension (5×10^5 spores mL^{-1}). Disease severity was assessed 14 days later by calculating the percentage of diseased spikelets per spike. All treatments consisted of at least three biological replicates, with representative plants selected for phenotypic recording and subsequent molecular analysis.

Statistical analysis

All experiments were performed with at least three independent biological replicates. Data were analyzed by one-way analysis of variance (ANOVA) followed by Tukey’s honestly significant difference (HSD) test ($p < 0.05$) using GraphPad Prism 9.0 software [28].

Results

Identification and characterization of TaND protein gene family members

To identify the NDs gene family in *T. aestivum*, a local Blast against the proteome of the *T. aestivum* was performed, and with the protein sequence of a member of the Arabidopsis AtND protein family as bait, we evaluated the conserved domains of the goal sequences and removed any redundant amino acid sequences using PHMMER and SMART online tools. 16 *ND* genes distributed on 9 chromosomes were identified in wheat. On the basis of subfamily classification and chromosomal localization, these 16 *NDs* in wheat were renamed, and detailed information, including gene structure and protein properties, is listed in Table 1, Table 2 and Table S1. The putative wheat ND proteins ranged from 343 to 620 amino acids in length, with theoretical molecular weights ranging from 36.9 to 68.7 kDa and theoretical

isoelectric points (pI) ranging from 6.47 to 9.29. The instability coefficient predicted that 12 of the ND proteins are stable.

Phylogenetic tree construction of the ND gene family

To study the evolution of the *ND* gene family, a phylogenetic tree was constructed of 29 *ND* genes from three species (*T. aestivum*, *Oryza sativa* and *Arabidopsis thaliana*) using the neighbor-joining (NJ) method (Table S2). Based on the topological structure of the phylogenetic tree, the *ND* genes of all investigated species are clearly divided into three distinct subfamilies, A-C, despite variations in gene copy numbers across species. In wheat, 6 *TaND* genes were corresponding to the *NDA* subfamily, 9 *TaND* genes were corresponding to the *NDB* subfamily, 1 *TaND* gene was corresponding to the NDC subfamily. It is well known that Hexaploid wheat contains three (A, B, and D) homoeologous subgenomes. Consequently, every hexaploid wheat gene potentially owns three homoeologs from three homoeologous chromosomes as a triad. Blast searches against the wheat genome revealed that the 16 *TaND* genes represented 16 homoeologs of 6 genes: *TaNDA* and *TaNDB* gene had all the three homoeologs, but *TaNDC* had only one homoeolog (Fig. 1). All three subfamilies of plant *ND* genes, *NDA*, *NDB* and *NDC* are present in wheat, but have fewer *NDB* genes than the well characterised in Arabidopsis.

The evolutionary history was inferred by using the Maximum Likelihood method based on 29 ND protein sequences. The bootstrap consensus tree inferred from 1000 replicates is taken to represent the evolutionary history of the taxa analyzed. The tree is condensed to show the three major subfamilies (A, B, and C), which are highlighted with different colored backgrounds. Thec associated TaND genes and their homoeologs are detailed in the main text. The analysis was conducted in MEGA X.

The evolutionary history was inferred by using the Maximum Likelihood method based on 29 ND protein sequences. The bootstrap consensus tree inferred from 1000 replicates is taken to represent the evolutionary history of the taxa analyzed. The tree is condensed to show the three major subfamilies (A, B, and C), which are highlighted with different colored backgrounds. The associated *TaND* genes and their homoeologs are detailed in the main text. The analysis was conducted in MEGA X.

Chromosome distribution analysis of the TaND genes

The *TaND* genes distribution within the wheat chromosomes was analyzed. The findings revealed that nine of the 42 chromosomes had an uneven distribution of the 16 *TaND* homoeologs (Fig. 2, Table S3). *TaNDA4-6* are located on chromosome 2. *TaNDA1-3* and *TaNDB4-6* are located on chromosome 3, *TaNDB1-3*, *TaNDB7-9* and *TaNDC1* are located on chromosome 7. Genomic distribution analysis revealed that 5 of the 6 *ND* genes maintain complete homoeologous sets across the A, B and D subgenomes, with *TaNDC1* being the sole exception as a 7D-specific single-copy gene.

The 16 *TaND* homoeologs were distributed on 9 chromosomes. *TaNDA2* was located on chr2; *TaNDA1* and *TaNDB2* on chr3; *TaNDB1*, *TaNDB3* and *TaNDC1* on chr7. Five genes maintained complete A, B, D homoeologous sets, while *TaNDC1* was a single-copy gene specific to chr7D.

The 16 *TaND* homoeologs were distributed on 9 chromosomes. *TaNDA2* was located on chr2; *TaNDA1* and *TaNDB2* on chr3; *TaNDB1*, *TaNDB3* and *TaNDC1* on chr7. Five genes maintained complete A, B, D homoeologous sets, while *TaNDC1* was a single-copy gene specific to chr7D.

Gene structure and motif analysis of the TaND genes

To analyze the structural diversity of the *TaND* genes, we generated a schematic diagram of their gene structures using TBtools (Fig. 3A). Furthermore, conserved motifs within the encoded proteins were predicted using the MEME suite. In total, twelve distinct motifs were identified across the *TaND* family (Fig. 3B).The motif composition was highly conserved among genes within the same subfamily. Among them, *TaNDB4* and *TaNDB6-9* genes contain the all 12 motifs, however, the *TaNDB5* gene lacks motif 11 compared with its homologues (*TaNDB4* and *TaNDB6*) on the A and D genomes. All members of the *TaNDA* gene family contain an identical set of motifs, which included all motifs except for motif 9 and motif 12. Strikingly, *TaNDC1* exhibits the most simplified motif pattern, containing only motif 10 and motif 11, which may indicate substantial functional divergence from other subfamilies.

Conserved domain analysis further elucidated the functional divergence among TaND subfamilies (Fig. 3C). The TaNDA and TaNDB groups shared a core NADH dehydrogenase domain, while TaNDB proteins were characterized by an additional C-terminal domain related to regulatory function. In contrast, TaNDC1 exhibited a distinctly simplified and unique domain architecture, lacking several domains present in both NDA and NDB groups, consistent with its early phylogenetic isolation and suggesting potential functional specialization.

The composition and function of genes are more diversified by changes in intron numbers, which are frequently observed during evolution. Differences in the patterns of exons and introns are important for evolution. The *TaND* genes had 0–3 UTR, according to our analysis of their exon/intron mappings (Fig. 3D). *TaNDC1* do not have UTR. *TaNDB2* and *TaNDB4-9* have nine introns. *TaNDB1* and *TaNDB3* have ten introns. *TaNDA1* and *TaNDA2* have seven introns, but *TaNDA3* have eight introns. *TaNDA4-6* have five introns, *TaNDC1* have six introns. The members listed above are part of the intron enrichment group (Fig. 3D). The structural simplicity of *TaNDC1* in both motif composition and gene architecture further supports its divergent evolution within the TaND family.

(A) The phylogenetic tree was constructed using the neighbor-joining method with 1,000 bootstrap replicates by MEGA X. (B) The motif composition of TaND proteins. The motif compositions of TaND proteins. The 12 motifs were indicated by colored boxes and numbered 1–12. (C) Conserved domain structure of TaNDs. Different colored blocks represent distinct conserved domains. (D) Exon–intron and UTR structure of *TaNDs*. Green boxes indicate UTRs, yellow boxes indicate CDS (coding sequences), and black lines indicate introns.

The Cis-regulatory elements analysis of TaND genes

To investigate the transcriptional regulation of *TaND* genes, Using PlantCARE software to analyze the promoter region of 16 *TaND* homoeologs (Fig. 4, Table S4 and Table S5), hormone responsive elements were identified, including methyl jasmonate responsive element (MeJA), abscisic acid responsive element (ABRE), gibberellin responsive element (GARE), salicylic acid responsive element TCA and auxin-responsive element (TGA); The stress response elements are low temperature response elements, drought response elements, light responsive element (LRE), anaerobic response elements, and anoxic specific inducibility elements, respectively; And growth related *cis*-acting elements involved in meristem expression, zein metabolism regulation, MYBHv1 binding site, endosperm expression regulation, and cell cycle regulation. Among these, the MeJA-responsive element and the light-responsive element (LRE) were found in all 16 promoters. In terms of stress response, LRE was present in all 16 *TaND* homologs, 6 *TaND* homoeologs had low temperature response regions, 12 *TaND* homoeologs had drought response regions, 12 *TaND* homoeologs had anaerobic induction or anoxic specific inducibility regions. And 9 of the 16 *TaND* homoeologs had MYBHv1 binding site. The presence of *cis*-acting elements in the promoter region suggested that the *TaND* gene family may be involved in the regulation of hormonal balance, response to stress, and wheat growth and development.

(A) Phylogenetic tree of *TaND* genes. (B) Distribution of cis - acting elements in *TaND* gene promoters, with different colors representing various elements (e.g., hormone - responsive, stress - responsive, growth - related). (C) Heatmap showing the abundance of different cis - acting elements in TaND gene promoters. PlantCARE analysis revealed multiple regulatory elements involved in hormone response, stress response, and growth regulation, implying TaND genes' roles in hormonal balance, stress adaptation, and wheat development.

Synteny analysis of TaND genes

In addition to polyploidization, gene duplication represents a principal driver of gene family expansion throughout genome evolutionary processes [29]. We utilized TBtools to conduct intraspecies collinearity analysis on the *TaND* gene family members. the result showed that the 16 wheat *TaND* homoeologs genes constituted 12 pairs of collinear genes and only *TaNDC1* had no collinearity with other *TaND* family genes (Fig. 5A, Table S6). These results indicated that segmental duplication contributed to the evolution of the *TaND* gene family in the wheat genome. In order to further analyze gene duplication, the *TaND* genes of wheat were investigated for their collinearity with the *ND* genes of Arabidopsis, rice, and maize. The number of collinearity gene pairs in wheat and Arabidopsis, wheat and rice as well as wheat and maize, was 8, 11 and 12, respectively. Interestingly, these syntenic gene pairs were primarily clustered in the *NDA* and *NDB* subfamilies, while *TaNDC1* lacked syntenic counterparts in these compared species (Fig. 5B, Table S7). These results concluded that the wheat *TaNDC1* may play a potential role in wheat-specific adaptations, possibly through neofunctionalization during polyploidization.

Analysis of TaND gene family hormonal and stress expression patterns

The expression patterns of gene family members are helpful in predicting their potential biological functions. To elucidate the potential role of *TaNDs*, their expression patterns were studied by qRT-PCR. We analyzed expression patterns of *TaND* family genes under two hormonal treatments (methyl jasmonate, JA; and salicylic acid, SA), two abiotic stresses (drought and heat stress), and three biotic stresses (Powdery mildew Bgt; Fusarium crown rot, FCW and Fusarium head blight, FHB) (Fig. 6). Due to the high sequence similarity among the three homoeologs of each *TaND* gene in wheat, only one representative subgenome copy per gene was selected for quantitative analysis.

Under JA and SA treatments, five *TaND* genes showed significant expression responses, while *TaNDA6* remained unexpressed. JA induction triggered early up-regulation of *TaNDB1*, *TaNDB4* and *TaNDC1*, with *TaNDC1* exhibiting highly significant induction at 12h. In contrast, *TaNDA1* and *TaNDB7* were down-regulated over time. Under SA treatment, *TaNDB7* showed significant suppression at 12h followed by strong induction at 48h, whereas *TaNDC1* was generally suppressed. *TaNDB1* expression increased continuously and reached significance at 48h. These results reveal distinct pathway-specific patterns: JA activation involving *TaNDB1*, *TaNDB4* and *TaNDC1*, and SA response mediated by *TaNDA1*, *TaNDB1*, *TaNDB4* and *TaNDB7*. Notably, *TaNDC1* shows opposite regulatory patterns in response to JA and SA: its expression is upregulated by JA treatment but downregulated by SA treatment. This indicates that *TaNDC1* may function as a key regulatory node within the JA and SA signaling pathways (Fig. 6A, 6B).

Under abiotic stress, drought stress significantly induced three *TaNDs* expression responses, *TaNDB1*, *TaNDB4* and *TaNDC1*. Among them, *TaNDB1* and *TaNDC1* exhibited strong induction at 10 h, while *TaNDB4* showed a transient induction at 6 h, peaking before declining to levels below the baseline (Fig. 6C). Heat stress triggered responsive expression of four genes, *TaNDB1*, *TaNDB4*, *TaNDB7* and *TaNDC1*. All of them displayed a trend of initial upregulation followed by downregulation, however, with the exception of *TaNDB4*, their expression levels ultimately remained elevated compared to baseline. These results suggest that *TaND* genes play divergent roles in abiotic stress responses, with some showing sustained upregulation and others displaying rapid, transient induction, indicating functional diversification within the gene family (Fig. 6D).

Transcriptional profiling of the *TaND* gene family under biotic stress revealed distinct expression patterns among members. Among these genes, *TaNDB1*, *TaNDB4*, *TaNDB7* and *TaNDC1* exhibited similar responses following infection by Bgt and FCW, with their expression being strongly suppressed. *TaNDA1* showed no significant change in expression after Bgt infection, but was markedly induced at 12 h post-inoculation with FCW before returning to baseline levels by 48 h. In contrast, FHB infection triggered a distinctly different expression pattern in *TaND* genes, where all were either induced or remained unchanged. Intriguingly, the expression trends of *TaNDC1* after Bgt/FCW infection resembled those following SA treatment, while its expression dynamics after FHB infection aligned with those observed under JA treatment. This suggests that the expression of *TaNDC1* may be primarily regulated by SA during Bgt and FCW infection, whereas it may be predominantly controlled by JA during FHB infection (Fig. 6E, 6F, 6G).

Expression profiles of six TaND genes in response to jasmonic acid (JA; A), salicylic acid (SA; B), drought (C), heat (D), powdery mildew (E), Fusarium crown rot (F), and Fusarium head blight (G). Data were normalized to internal reference genes and represent the means of three biological replicates. Error bars indicate the standard deviation. Asterisks indicate significant differences compared to the control (assessed using Student's t-test), **P < 0.01. FHB, Fusarium head blight.

Silencing of TaND reduced the resistance of wheat to FHB

Previous studies have established that the JA signaling pathway is associated with resistance to FHB in wheat, and exogenous JA application can enhance resistance to FHB infection, as demonstrated in both wheat and other cereal crops [30]. Given that *TaNDC1* specifically responds to JA and is significantly upregulated under FHB stress, we hypothesized that this gene may play a functional role in FHB resistance. To test this, virus-induced gene silencing (VIGS) was performed in the resistant wheat cultivar Sumai 3. After 15 days, the positive control plants exhibited typical photobleaching phenotypes, confirming the successful establishment of the VIGS system. At the flowering stage, plants with silenced *TaNDC1* and control plants were inoculated with a spore suspension of *F. graminearum*. Quantitative analysis revealed more than 90% suppression of *TaNDC1* expression in silenced plants. Notably, silencing of *TaNDC1* significantly compromised FHB resistance in Sumai 3 (Fig. 7). These results collectively demonstrate that *TaNDC1* participates in the defense response and positively regulates resistance to FHB in wheat.

(A) The spike phenotype of BSMV:00-(control) and BSMV:TaNDC1-treated plants at 12 days post-inoculation with *F. graminearum*. (B) Relative expression level of *TaNDC1* in control and silenced plants. .Data are presented as mean ± SD from three independent biological replicates. (C) Disease index (DI) of BSMV:00 and BSMV:TaNDC1 wheat spikes at 7, 14 and 21dpi with *F. graminearum*. In boxplot, boxes represent the interquartile range, center lines indicate medians, and whiskers extend to the minima and maxima. **P < 0.01.

TaNDC1 interacts with TaPFT

FHB is a globally devastating wheat disease. To date, hundreds of quantitative trait loci (QTLs) for FHB resistance have been identified in wheat and its relatives. While the majority of their underlying genes remain uncloned, nine QTLs (*Fhb1-Fhb9*) have been formally named [31]. Among these, only *Fhb1* and *Fhb7* have been positionally cloned, both conferring significant resistance. The *Fhb7* gene, originating from the wild relative *Thinopyrum ponticum*, encodes a glutathione S-transferase (GST), possesses an exceptional ability to detoxify the trichothecene toxin deoxynivalenol (DON) by epoxidizing its critical C12/C13 epoxy group, thereby conferring resistance [32]. *Fhb1* was first identified in the Chinese wheat cultivar Sumai 3 and its derivative Ning 7840, and is now widely utilized in global FHB resistance breeding. Although the candidate genes *TaPFT* and *TaHRC* (also known as *TaHis*) have been proposed for this locus, some studies contest *TaPFT*'s role, and the precise resistance mechanism of *Fhb1* remains unresolved [33]. To investigate whether *TaNDC1* is associated with known, cloned FHB resistance genes in wheat, we selected *TaHRC* and *TaPFT* for further study. The *GST* gene (from *Fhb7*)

was not selected because it is exogenous and not present in common wheat. Using the yeast two-hybrid (Y2H) assay, we examined the interaction between TaNDC1 and TaHRC/TaPFT. The co-transformant yeast cells of BD-*TaPFT*/ AD-*TaNDC1* grew well and turned blue on the selective medium., whereas the co-transformant yeast cells of BD-*TaHRC*/AD-*TaNDC1* could not grow on SD/-Ade/-His/-Leu/-Trp/ABA/X-α-Gal media. This result demonstrated a specific interaction between *TaNDC1* and *TaPFT*, but not with *TaHRC*, in the yeast system (Fig. 8). To verify this experimental result, the *TaHRC* and *TaPFT* were ligated into the YFP-N (YN) vector, the *TaNDC1* was ligated into the YFP-C (YC) vector, respectively. The results of the BiFC assay showed that fluorescence was only detected in tobacco leaves co-expressing the YN-TaPFT + YC-TaNDC1 recombinant plasmid pair. In contrast, no fluorescence was observed in leaves co-expressing the YN-TaHRC + YC-TaNDC1 pair, as was the case with all other controls (Fig. 9). This demonstrates that TaNDC1 interacts with TaPFT, but not with TaHRC, in planta, which is consistent with the result from the yeast system. Also, an AutoDock software prediction was used to conclude that there is an interaction relationship between TaNDC1 and TaPFT (Fig. 10). All of the above results suggest that TaNDC1 and TaPFT interact physically in cells. However, whether this interaction is relevant to FHB resistance in wheat requires further investigation.

Experimental groups (pGBKT7 TaPFT + pGADT7 TaNDC1, pGBKT7 TaHRC + pGADT7 TaNDC1) were tested alongside negative controls (pGBKT7 Lam + pGADT7 T, pGBKT7 + pGADT7 NADPH, pGBKT7 TaPFT + pGADT7, pGBKT7 TaHRC + pGADT7) and a positive control (pGBKT7 53 + pGADT7 T). Yeast transformants were spotted on SD/ Trp/ Leu and SD/ Trp/ Leu/ Ade/ His media supplemented with ABA and X α Gal. Serial dilutions (1, 10^{-1}, 10^{-2}, 10^{-3}) are shown.

The experimental groups (YN-TaHRC + YC-TaNDC1,YN-TaPFT + YC-TaNDC1) and the negative controls (YN-TaPFT + YC, YN + YC-TaNDC1,YN-TaHRC + YC) were showed. Representative images from left to right show YFP fluorescence (YFP), bright-field view (Bright), and the merged channel (Merge).

Discussion

Wheat, as a crucial cereal crop, requires thorough functional characterization of its gene families to elucidate its response mechanisms to environmental and stress. The *ND* family represents a core component of the alternative respiratory pathway in plant mitochondria. This gene family plays a pivotal role in regulating redox homeostasis, energy metabolism, and responses to stress, functions that have been well established across diverse plant species [2, 34]. However, the evolutionary patterns and functional differentiation of this family in polyploid wheat have not been systematically elucidated. Through genome-wide identification, this study identified 16 *TaND* genes in wheat, which were classified into three subfamilies: *NDA*, *NDB*, and *NDC*. The number of *TaND* genes is significantly higher than that in Arabidopsis and rice, which have 7 and 6 members, respectively, reflecting the expansion of the gene family during allopolyploidization—a genomic phenomenon commonly observed in wheat evolution [7]. Chromosomal localization analysis revealed that *TaND* genes are evenly distributed across nine chromosomes. Most core genes, including *TaNDA1–6* and *TaNDB1–9*, form complete homoeologous triads across the A, B, and D subgenomes, suggesting a conserved mechanism for maintaining gene

dosage balance to support fundamental metabolic functions. This absence indicates possible functional specialization through subgenome-specific gene loss, an evolutionary process documented in previous polyploid wheat studies [35]. Furthermore, collinearity analysis indicated that segmental duplication serves as the primary mechanism for the expansion of the *TaND* family. *TaNDC1*, however, exhibits no collinearity with other members within wheat and lacks conserved orthologs in cross-species comparisons. These observations further support the hypothesis that *TaNDC1* has undergone functional divergence during evolution.

Gene structure and conserved domain analysis revealed that members of the *TaNDB* and *TaNDA* subfamilies contain 12 and 10 conserved motifs respectively, all possessing typical NADH dehydrogenase domains along with additional regulatory domains such as PTZ00318, EF-hand, and PTZ00183 superfamilies. In contrast, *TaNDC1* retains only two conserved motifs (Motif 10 and 11) and lacks multiple key domains, demonstrating significant structural simplification. Its gene structure is further characterized by the absence of UTR regions and a reduced number of introns (6), markedly fewer than other members (7–10 introns), indicating that *TaNDC1* may have transitioned to a more specialized biological role, as documented in studies of gene family evolution [5, 36]. Promoter cis-element analysis showed that all *TaND* members contain MeJA and LREs, with the *NDB* subfamily enriched in hormone and stress-responsive elements and the *NDA* subfamily associated with growth and development. Compared to other *TaNDs*, *TaNDC*1 lacks many cis-regulatory elements and contains only LRE, MeJA, ABRE, TGA, GARE, and meristem expression, with primary enrichment observed in LRE and MeJA, while lacking growth-related elements, suggesting its specific involvement in relevant stress responses. The compositional differences in these regulatory elements reflect the adaptive stress environments during wheat polyploidization and provide transcriptional evidence for the functional specificity of *TaNDC1*.

To validate the functional specificity of the *TaND* family in stress resistance and hormonal responses, this study investigated their expression patterns under two hormones (JA and SA), two abiotic stresses (drought and heat) and three biotic stresses (Bgt, FCW and FHB). All *NDs* genes exhibited responses to at least one of the aforementioned treatments, aligning with their established role in plant environmental adaptation. In comparison, *NDBs* and *NDC1* were involved in responses to a broader range of the aforementioned treatments than *NDAs.* Although promoter analysis of *TaNDA4* revealed the presence of 9 ABREs and 8 MeJAs, no significant expression change was observed under drought treatment (primarily regulated by ABA) or JA treatment. This may be attributed to the predominant responsiveness of *TaNDA4* to high-light treatment, as its promoter contains as many as 15 LREs. Notably, *TaNDC1* exhibited broad responsiveness to almost all of the above treatments. In particular, it showed contrasting responses to JA and SA hormone treatments, with JA inducing its expression and SA suppressing it. It is well established that the JA and SA pathways play pivotal roles in plant defense against pathogen infection. Typically, these two signaling pathways exhibit an antagonistic interaction within plants, whereby activation of the SA pathway often suppresses the JA pathway, and vice versa [37, 38]. Previous studies have shown that during FHB infection in wheat, JA antagonizes SA signaling at the

early infection stage, leading to a decrease in SA levels and consequently a reduction in FHB resistance. In contrast, during the later stages of infection, JA shifts to a predominant role, enhancing resistance to FHB [39]. In this study, expression profiling demonstrated that *TaNDC1* was markedly induced at 12 h after JA treatment, while showing sustained suppression under SA treatment, indicating specific responsiveness to JA signals consistent with the established role of JA in mediating resistance to FHB. Virus-induced gene silencing in the resistant cultivar Sumai 3 confirmed its biological function, as silenced plants exhibited significantly expanded lesion areas with transcript levels substantially reduced compared to controls, demonstrating a clear susceptible phenotype and confirming *TaNDC1* as a positive regulator in FHB resistance. These results suggest that *TaNDC1* may be involved in FHB defense through JA and SA signal perception or transduction, and its functional specialization reflects the adaptive evolutionary process during the polyploidization of wheat [40].

FHB, primarily caused by the hemibiotrophic fungus *Fusarium graminearum*, exhibits an initial biotrophic phase followed by a necrotrophic phase. During the biotrophic stage, both ROS and programmed cell death (PCD) contribute to restricting fungal infection. In contrast, during the necrotrophic stage, the accumulation of ROS and induction of PCD conversely facilitate pathogen progression. Transcriptomic analysis of highly resistant (AAC Tenacious) and highly susceptible (Wilkin) wheat cultivars to FHB revealed that effective resistance is associated with the downregulation or restriction of two key defense-related pathways: PCD and the generation/accumulation of ROS [41]. The alternative respiratory pathway composed of *NDs* and *AOXs* in plant mitochondria serves as a significant bypass to the classical, energy-conserving electron transport chain (ETC) [42, 43]. Compelling evidence indicates that AP activity alleviates over-reduction of the ETC. Functioning as an overflow mechanism, the AP is thought to confer metabolic flexibility under environmental stress and has been shown to attenuate ROS production, particularly when the capacity of the classical ETC is impaired [8, 44, 45]. Although direct evidence linking *TaNDC1* to ROS generation is currently lacking in this study, we hypothesize that *TaNDC1*, as a typical type II NAD(P)H dehydrogenase, may contribute to FHB resistance by modulating ROS accumulation and the associated PCD. Additionally, in this study, we demonstrate an interaction between TaNDC1 and TaPFT. Although some studies have refuted the role of *TaPFT* in FHB resistance [46, 47], other reports indicate that heterologous expression of *TaPFT* in *Arabidopsis* confers broad-spectrum resistance to fungal pathogens, including *Fusarium graminearum* [48]. Whether the interaction between TaNDC1 and TaPFT is relevant to wheat resistance against FHB requires further experimental investigation.

Conclusion

In this study, we identified 16 *NDs* in wheat through genome-wide identification and were classified into three subfamilies: NDA, NDB, and NDC. Expression analysis indicated that *TaNDs* genes play roles in response to environmental stresses and are regulated by hormones. We further screened *TaNDC1* as the most responsive gene to FHB, showing JA-induced but SA-suppressed expression. Silencing *TaNDC1* in wheat significantly compromised resistance to FHB. Further protein interaction assays confirmed that

TaNDC1 physically interacts with TaPFT. Collectively, these results delineate key characteristics of the *TaND* gene family, establish *TaNDC1* as a critical player in FHB resistance, and provide a foundation for further study of TaND proteins. Importantly, this work positions *TaNDC*1 as a promising target for breeding FHB-resistant wheat varieties with practical potential to enhance disease resilience in agriculture.

Declarations

Ethics approval and consent to participate

Not applicable.

Consent for publication

Not applicable.

Competing interests

The authors declare no competing interests.

Funding

This work was funded by the Key Scientific Research Projects of Colleges and Universities in Henan Province (26A210005) and Key Research and Development Project of Henan Province (261111113200).

Author Contribution

PS and ZR conceived and designed the experiments. LW, AL, DL and YL performed the experiments. LW, AL, PH, YG , MZand QL performed the data analyses. PS, LW and AL wrote the manuscript. HH and ZR revised the manuscript. All authors have read and approved the final version of the manuscript.

Acknowledgements

We would like to thank the reviewers for their helpful comments on the original manuscript.

Availability of data and materials

All data generated or analyzed during this study are included in this article and can be found in supplementary files Table S1-S8

References

1. Millar HA, Whelan J, ,Soole LK, et al. Organization and regulation of mitochondrial respiration in plants. Annu Rev Plant Biol. 2011;62:79–104.
2. Vanlerberghe GC. Alternative oxidase: a mitochondrial respiratory pathway to maintain metabolic and signaling homeostasis during abiotic and biotic stress in plants. Int J Mol Sci. 2013;14(4):6805–47.
3. Wanniarachchi VR, Dametto L, Sweetman C, et al. Alternative Respiratory Pathway Component Genes (AOX and ND) in Rice and Barley and Their Response to Stress. Int J Mol Sci. 2018;19(3):915.
4. Moore CS, Cook-Johnson RJ, Rudhe C, et al. Identification of AtNDI1, an internal non-phosphorylating NAD(P)H dehydrogenase in Arabidopsis mitochondria. Plant Physiol. 2003;133(4):1968–78.
5. Elhafez D, Murcha MW, et al. Characterization of mitochondrial alternative NAD(P)H dehydrogenases in Arabidopsis: intraorganelle location and expression. Plant Cell Physiol. 2006;47(1):43–54.
6. Sweetman C, Waterman CD, Rainbird BM, et al. AtNDB2 Is the Main External NADH Dehydrogenase in Mitochondria and Is Important for Tolerance to Environmental Stress. Plant Physiol. 2019;181(2):774–88.
7. Michalecka AM, Svensson AS, Johansson FI, et al. Arabidopsis genes encoding mitochondrial type II NAD(P)H dehydrogenases have different evolutionary origin and show distinct responses to light. Plant Physiol. 2003;133(2):642–52.
8. Jethva J, Lichtenauer S, Schmidt-Schippers R, et al. Mitochondrial alternative NADH dehydrogenases NDA1 and NDA2 promote survival of reoxygenation stress in Arabidopsis by safeguarding photosynthesis and limiting ROS generation. New Phytol. 2023;238(1):96–112.
9. Wallström SV, Florez-Sarasa I, Araújo WL, et al. Suppression of the external mitochondrial NADPH dehydrogenase, NDB1, in Arabidopsis thaliana affects central metabolism and vegetative growth. Mol Plant. 2014;7(2):356–68.
10. Smith C, Barthet M, Melino V, et al. Alterations in the mitochondrial alternative NAD(P)H Dehydrogenase NDB4 lead to changes in mitochondrial electron transport chain composition, plant growth and response to oxidative stress. Plant Cell Physiol. 2011;52(7):1222–37.
11. Fatihi A, Latimer S, Schmollinger S, et al. A Dedicated Type II NADPH Dehydrogenase Performs the Penultimate Step in the Biosynthesis of Vitamin K1 in Synechocystis and Arabidopsis. Plant Cell. 2015;27(6):1730–41.
12. Marcussen T, Sandve SR, Heier L, et al. Ancient hybridizations among the ancestral genomes of bread wheat. Science. 2014;345(6194):1250092.
13. Boutigny A, Ward JT, ,Ballois N, et al. Diversity of the *Fusarium graminearum* species complex on French cereals[J]. Eur J Plant Pathol. 2014;138(1):133–48.
14. Pestka JJ. Deoxynivalenol: mechanisms of action, human exposure, and toxicological relevance. Arch Toxicol. 2010;84(9):663–79.

15. Schultz J, Copley RR, Doerks T, et al. SMART: a web-based tool for the study of genetically mobile domains. Nucleic Acids Res. 2000;28(1):231–4.
16. Finn RD, Bateman A, Clements J, et al. Pfam: the protein families database. Nucleic Acids Res. 2014;42(Database issue):D222–30.
17. Wilkins MR, Gasteiger E, Bairoch A, et al. Protein identification and analysis tools in the ExPASy server. Methods Mol Biol. 1999;112:531–52.
18. Walker JMT. Proteom Protocols Handbook[J] Humana Press, 2005, 1013851592598900.
19. Sievers F, Wilm A, Dineen D, et al. Fast, scalable generation of high-quality protein multiple sequence alignments using Clustal Omega. Mol Syst Biol. 2011;7:539.
20. Tamura K, Peterson D, Peterson N, et al. MEGA5: molecular evolutionary genetics analysis using maximum likelihood, evolutionary distance, and maximum parsimony methods. Mol Biol Evol. 2011;28(10):2731–9.
21. Chen C, Chen H, Zhang Y, et al. TBtools: An Integrative Toolkit Developed for Interactive Analyses of Big Biological Data. Mol Plant. 2020;13(8):1194–202.
22. Bailey TL, Johnson J, Grant CE, et al. The MEME Suite. Nucleic Acids Res. 2015;43(W1):W39–49.
23. Chen Y, Song W, Xie X, et al. A Collinearity-Incorporating Homology Inference Strategy for Connecting Emerging Assemblies in the Triticeae Tribe as a Pilot Practice in the Plant Pangenomic Era. Mol Plant. 2020;13(12):1694–708.
24. Chao J, Li Z, Sun Y, et al. MG2C: a user-friendly online tool for drawing genetic maps. Mol Hortic. 2021;1(1):16.
25. Lescot M, Déhais P, Thijs G, et al. PlantCARE, a database of plant cis-acting regulatory elements and a portal to tools for in silico analysis of promoter sequences. Nucleic Acids Res. 2002;30(1):325–7.
26. Morris GM, Huey R, Olson AJ. Using AutoDock for ligand-receptor docking. *Curr Protoc Bioinformatics*. 2008;Chap. 8.
27. DeLano WL, Pymol. An open-source molecular graphics tool. CCP4 Newsl. protein crystallogr. 2002;40(1):82–92.
28. Sakuraba Y, Bülbül S, Piao W, et al. Arabidopsis EARLY FLOWERING3 increases salt tolerance by suppressing salt stress response pathways. Plant J. 2017;92(6):1106–20.
29. Cannon SB, Mitra A, Baumgarten A, et al. The roles of segmental and tandem gene duplication in the evolution of large gene families in Arabidopsis thaliana. BMC Plant Biol. 2004;4:10.
30. Bigini V, Sillo F, Giulietti S, et al. Oligogalacturonide application increases resistance to Fusarium head blight in durum wheat. J Exp Bot. 2024;75(10):3070–91.
31. Zhang F, Zhang H, Liu J et al. Fhb9, a major QTL for Fusarium head blight resistance improvement in wheat[J]. J Integr Agric. 2024.
32. Wang H, Sun S, Ge W, et al. Horizontal gene transfer of *Fhb7* from fungus underlies *Fusarium* head blight resistance in wheat. Science. 2020;368(6493):eaba5435.

33. Ma H, Liu Y, Zhang S, et al. Wheat resistance to Fusarium head blight and breeding strategies[J]. Crop Health. 2025;3(1):1–11.
34. Rasmusson AG, Soole KL, Elthon TE. Alternative NAD(P)H dehydrogenases of plant mitochondria. Annu Rev Plant Biol. 2004;55:23–39.
35. Wang X, Yan X, Hu Y, et al. A recent burst of gene duplications in Triticeae. Plant Commun. 2021;3(2):100268. Published 2021 Dec 11.
36. Jiang WK, Liu YL, Xia EH, Gao LZ. Prevalent role of gene features in determining evolutionary fates of whole-genome duplication duplicated genes in flowering plants. Plant Physiol. 2013;161(4):1844–61.
37. Zheng XY, Spivey NW, Zeng W, et al. Coronatine promotes Pseudomonas syringae virulence in plants by activating a signaling cascade that inhibits salicylic acid accumulation. Cell Host Microbe. 2012;11(6):587–96.
38. Fang X, Chai W, Li S, et al. HSP17.4 mediates salicylic acid and jasmonic acid pathways in the regulation of resistance to Colletotrichum gloeosporioides in strawberry. Mol Plant Pathol. 2021;22(7):817–28.
39. Makandar R, Nalam VJ, Lee H, Trick HN, Dong Y, Shah J. Salicylic acid regulates basal resistance to Fusarium head blight in wheat. Mol Plant Microbe Interact. 2012;25(3):431–9.
40. Wu Y, Feng J, Zhang Q, et al. Integrative gene duplication and genome-wide analysis as an approach to facilitate wheat reverse genetics: An example in the TaCIPK family. J Adv Res. 2024;61:19–33.
41. Seifi S, Kaviani M, Navabi A, et al. Underlying mechanisms of FHB susceptibility and resistance in wheat: Insights from a transcriptome-based analysis[J]. Crop Sci. 2023;63(4):2347–70.
42. Vercesi AE, Borecký J, Maia Ide G, et al. Plant uncoupling mitochondrial proteins. Annu Rev Plant Biol. 2006;57:383–404.
43. Møller IM, Rasmusson AG, Van Aken O. Plant mitochondria - past, present and future. Plant J. 2021;108(4):912–59.
44. Vishwakarma A, Tetali SD, Selinski J et al. Importance of the alternative oxidase (AOX) pathway in regulating cellular redox and ROS homeostasis to optimize photosynthesis during restriction of the cytochrome oxidase pathway in Arabidopsis thaliana.
45. Popov VN, Syromyatnikov MY, Fernie AR, et al. The uncoupling of respiration in plant mitochondria: keeping reactive oxygen and nitrogen species under control. J Exp Bot. 2021;72(3):793–807.
46. Yan L, Tian J, Li J, et al. Analysis of a Series of Mutants Highlights Complex Regulation of Fusarium Head Blight Resistance Conferred by Fhb1 Locus in Wheat. Plant Biotechnol J. 2025;23(12):5891–3.
47. Shi J, Kong Z, Zhong J, et al. Mutagenesis and analysis of contrasting wheat lines do not support a role for PFT in Fusarium head blight resistance. Nat Genet. 2025;57(2):310–3.
48. Singh L, Sinha A, Gupta M, et al. Wheat Pore-Forming Toxin-Like Protein Confers Broad-Spectrum Resistance to Fungal Pathogens in *Arabidopsis*. Mol Plant Microbe Interact. 2023;36(8):489–501.

Tables

Tables 1 and 2 are available in the Supplementary Files section.

Figures

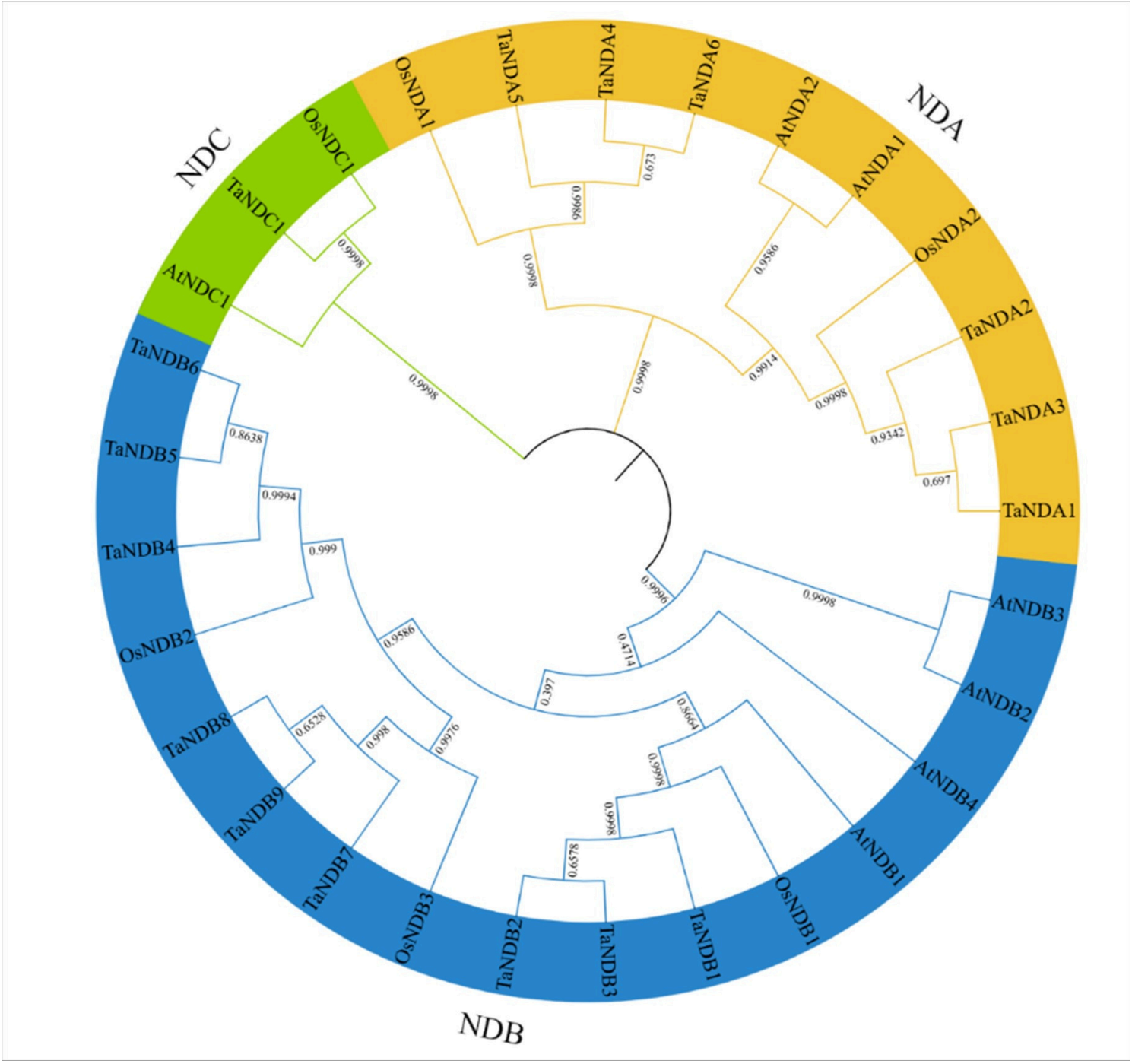


Figure 1

Phylogenetic analysis of ND genes from wheat, rice, and Arabidopsis thaliana.
The evolutionary history was inferred by using the Maximum Likelihood method based on 29 ND protein

sequences. The bootstrap consensus tree inferred from 1000 replicates is taken to represent the evolutionary history of the taxa analyzed. The tree is condensed to show the three major subfamilies (A, B, and C), which are highlighted with different colored backgrounds. The associated *TaND*genes and their homoeologs are detailed in the main text. The analysis was conducted in MEGA X.

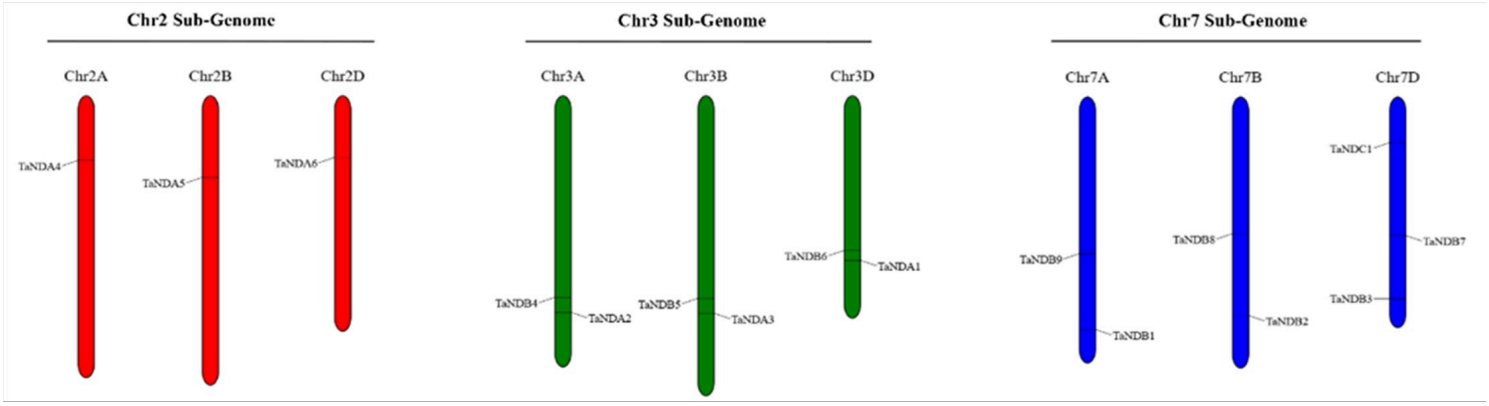


Figure 2

Chromosomal distribution of *TaND*genes.

The 16 *TaND* homoeologs were distributed on 9 chromosomes. *TaNDA2* was located on chr2; *TaNDA1* and *TaNDB2* on chr3; *TaNDB1*, *TaNDB3* and *TaNDC1* on chr7. Five genes maintained complete A, B, D homoeologous sets, while *TaNDC1* was a single-copy gene specific to chr7D.

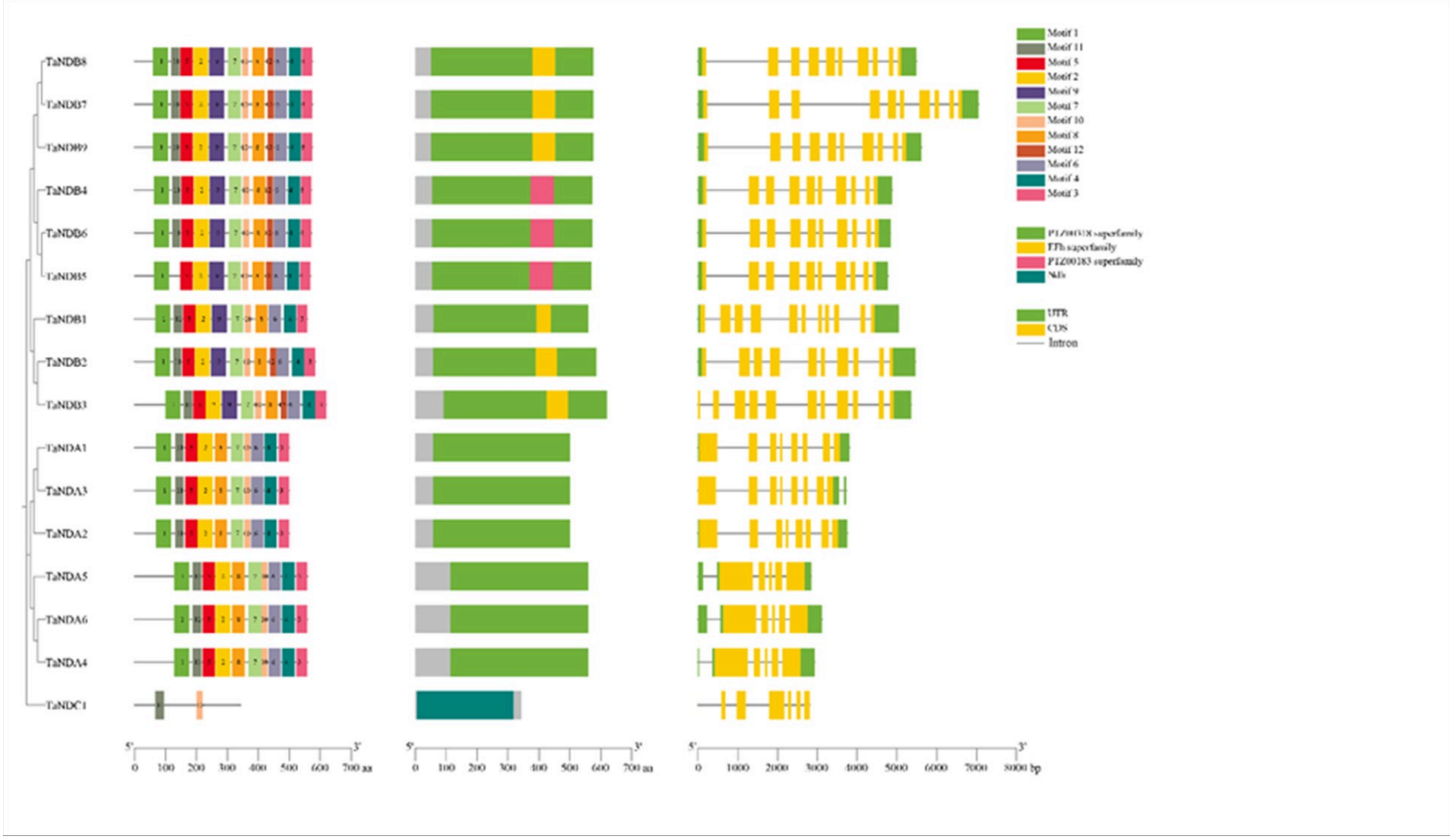


Figure 3

Phylogenetic relationships, conserved motifs, conserved domains, and gene structure of *TaND* genes in wheat.

(A) The phylogenetic tree was constructed using the neighbor-joining method with 1,000 bootstrap replicates by MEGA X. (B) The motif composition of TaND proteins. The motif compositions of TaND proteins. The 12 motifs were indicated by colored boxes and numbered 1–12. (C) Conserved domain structure of TaNDs. Different colored blocks represent distinct conserved domains. (D) Exon–intron and UTR structure of *TaNDs*. Green boxes indicate UTRs, yellow boxes indicate CDS (coding sequences), and black lines indicate introns.

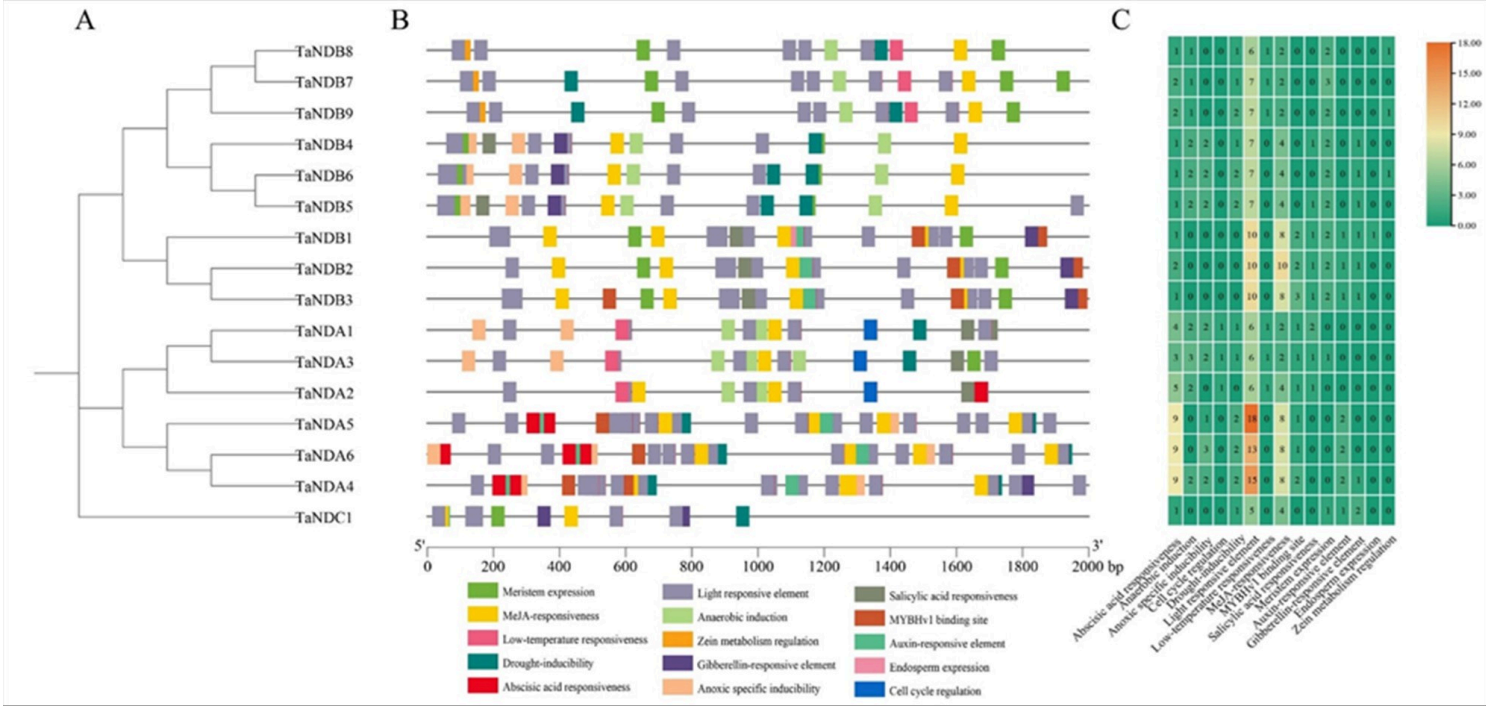


Figure 4

Promoter cis - acting regulatory elements of TaND genes.

(A) Phylogenetic tree of *TaND*genes. (B) Distribution of cis - acting elements in *TaND* gene promoters, with different colors representing various elements (e.g., hormone - responsive, stress - responsive, growth - related). (C) Heatmap showing the abundance of different cis - acting elements in TaND gene promoters. PlantCARE analysis revealed multiple regulatory elements involved in hormone response, stress response, and growth regulation, implying TaND genes' roles in hormonal balance, stress adaptation, and wheat development.

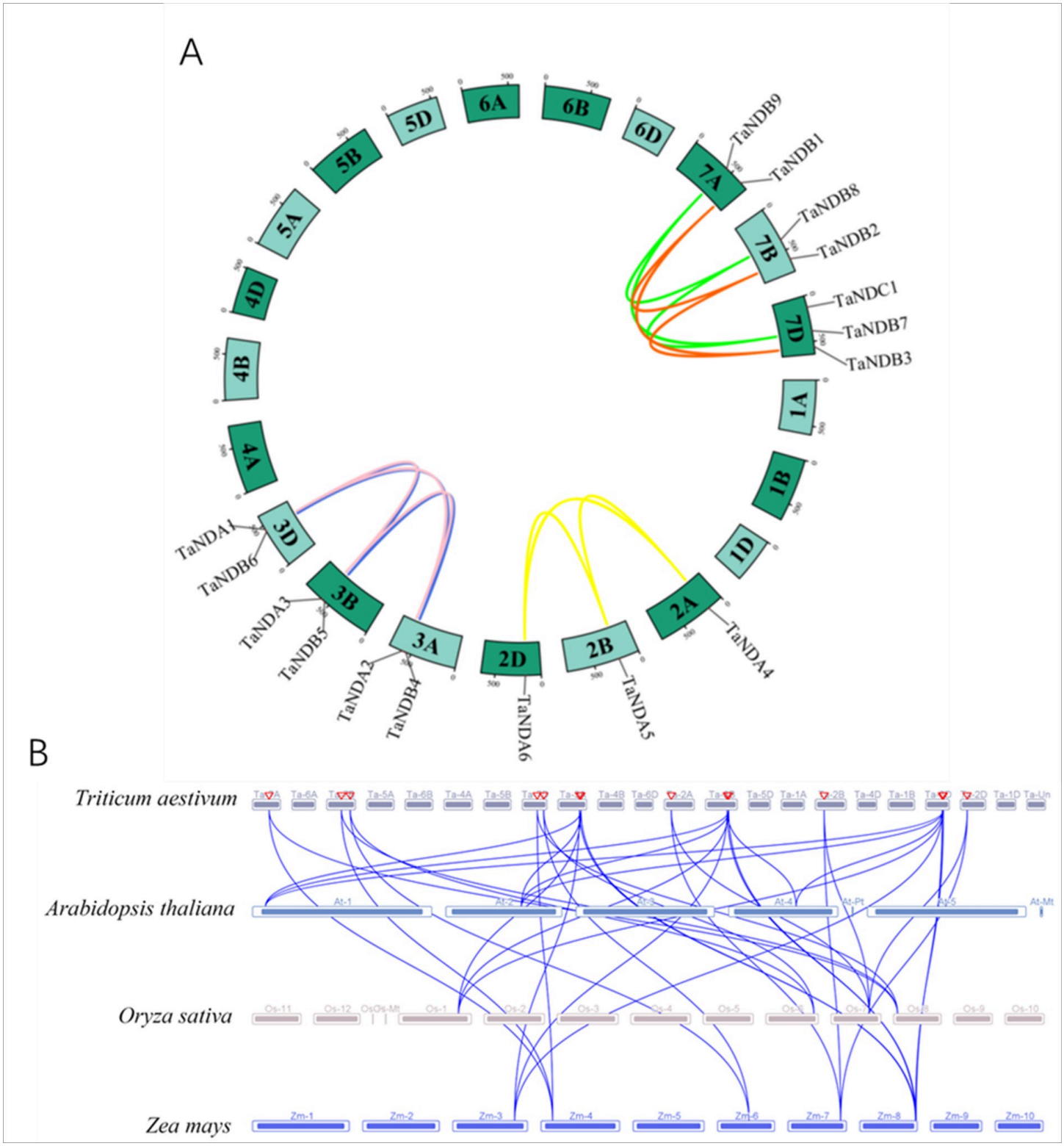


Figure 5

Synteny analysis of the *TaND* gene family.

(A) Intraspecies synteny analysis of *TaND* genes in *Triticum aestivum*. Colored lines indicate collinear gene pairs. Sixteen wheat *TaND*homoeologs form 12 collinear pairs, whereas *TaNDC1* exhibits no synteny with other *TaND* genes, suggesting segmental duplication contributed to *TaND* family expansion in wheat.

(B) Interspecies synteny analysis of *TaND* genes with *ND* genes from *Arabidopsis thaliana*, *Oryza sativa*, and *Zea mays*. Blue lines represent collinear pairs. The number of syntenic gene pairs between wheat and *A. thaliana*, *O. sativa*, and *Z. mays* is 8, 11, and 12, respectively. These pairs are primarily clustered in the *NDA* and *NDB* subfamilies. *TaNDC1*has no syntenic counterparts in these species, implying a potential role in wheat-specific adaptation, possibly through neofunctionalization during polyploidization. Black lines indicate 1-to-1 mutual best hits.

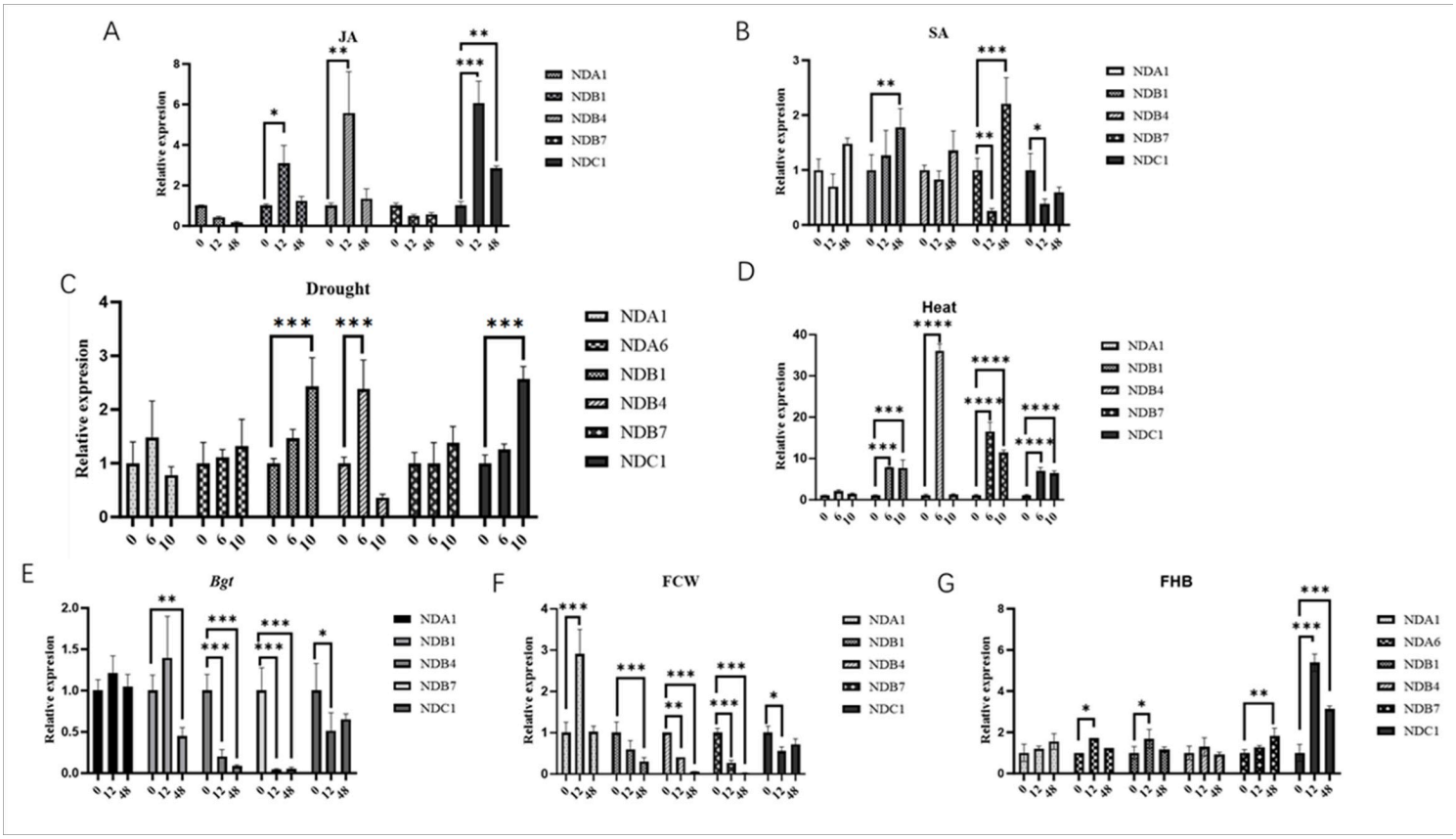


Figure 6

Relative expression levels of TaND genes under hormonal and stress treatments.
Expression profiles of six TaND genes in response to jasmonic acid (JA; A), salicylic acid (SA; B), drought (C), heat (D), powdery mildew (E), Fusarium crown rot (F), and Fusarium head blight (G). Data were normalized to internal reference genes and represent the means of three biological replicates. Error bars indicate the standard deviation. Asterisks indicate significant differences compared to the control (assessed using Student's t-test), **P < 0.01. FHB, Fusarium head blight.

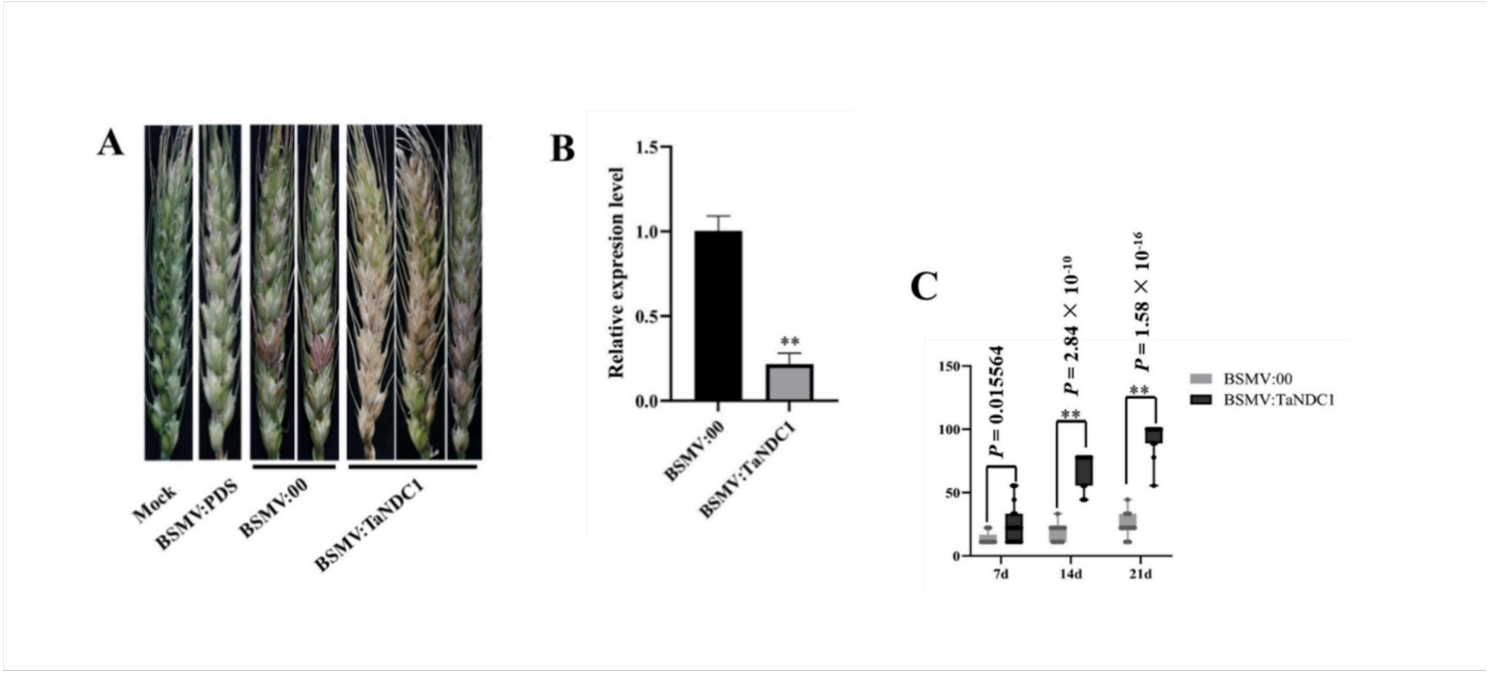


Figure 7

Effects of *TaNDC1* silencing by BSMV-VIGS in wheat cultivar Sumai 3 and related assessment.

(A) The spike phenotype of BSMV:00-(control) and BSMV:TaNDC1-treated plants at 12 days post-inoculation with *F. graminearum*. (B) Relative expression level of *TaNDC1* in control and silenced plants. .Data are presented as mean ±SD from three independent biological replicates. (C) Disease index (DI) of BSMV:00 and BSMV:TaNDC1 wheat spikes at 7, 14 and 21dpi with *F. graminearum*. In boxplot, boxes represent the interquartile range, center lines indicate medians, and whiskers extend to the minima and maxima. **P < 0.01.

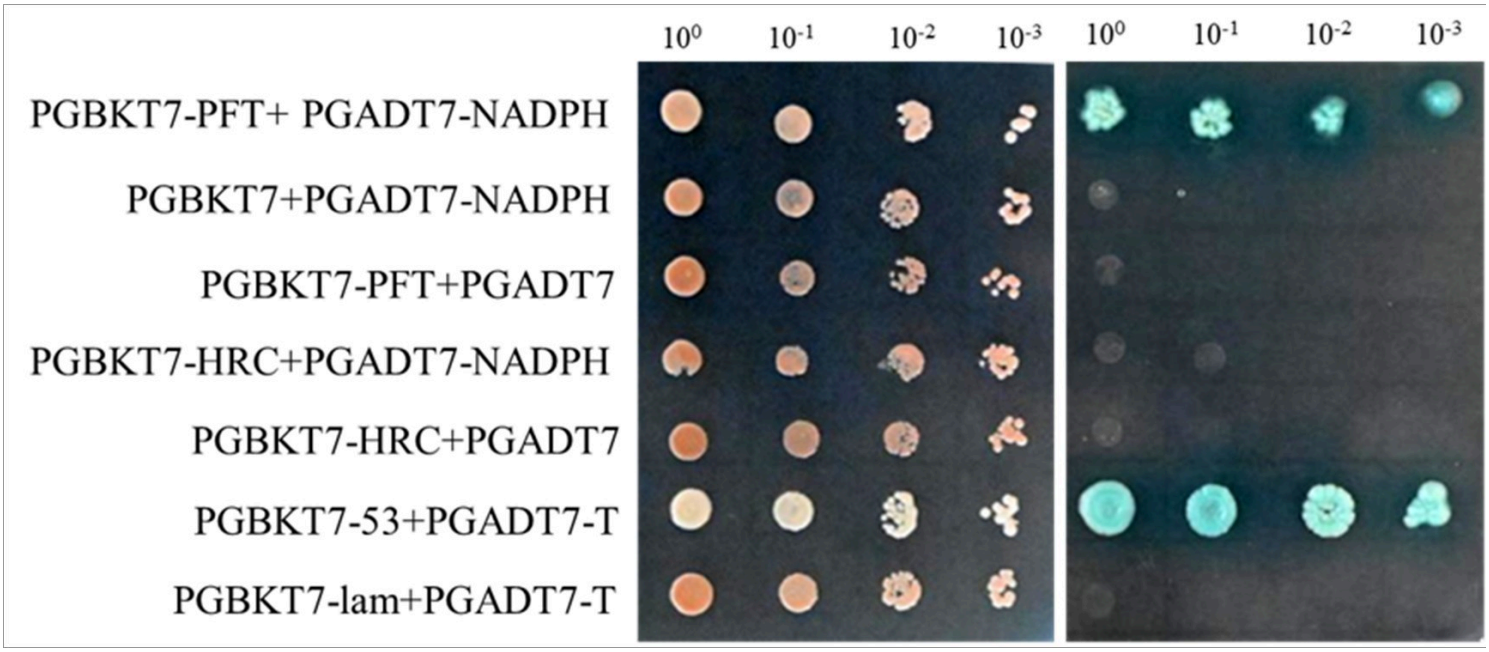


Figure 8

Yeast two hybrid analysis of the interaction between TaNDC1 and TaPFT/TaHRC.

Experimental groups (pGBKT7 TaPFT + pGADT7 TaNDC1, pGBKT7 TaHRC + pGADT7 TaNDC1) were tested alongside negative controls (pGBKT7 Lam + pGADT7 T, pGBKT7 + pGADT7 NADPH, pGBKT7 TaPFT + pGADT7, pGBKT7 TaHRC + pGADT7) and a positive control (pGBKT7 53 + pGADT7 T). Yeast transformants were spotted on SD/ Trp/ Leu and SD/ Trp/ Leu/ Ade/ His media supplemented with ABA and X α Gal. Serial dilutions (1, 10^{-1}, 10^{-2}, 10^{-3}) are shown.

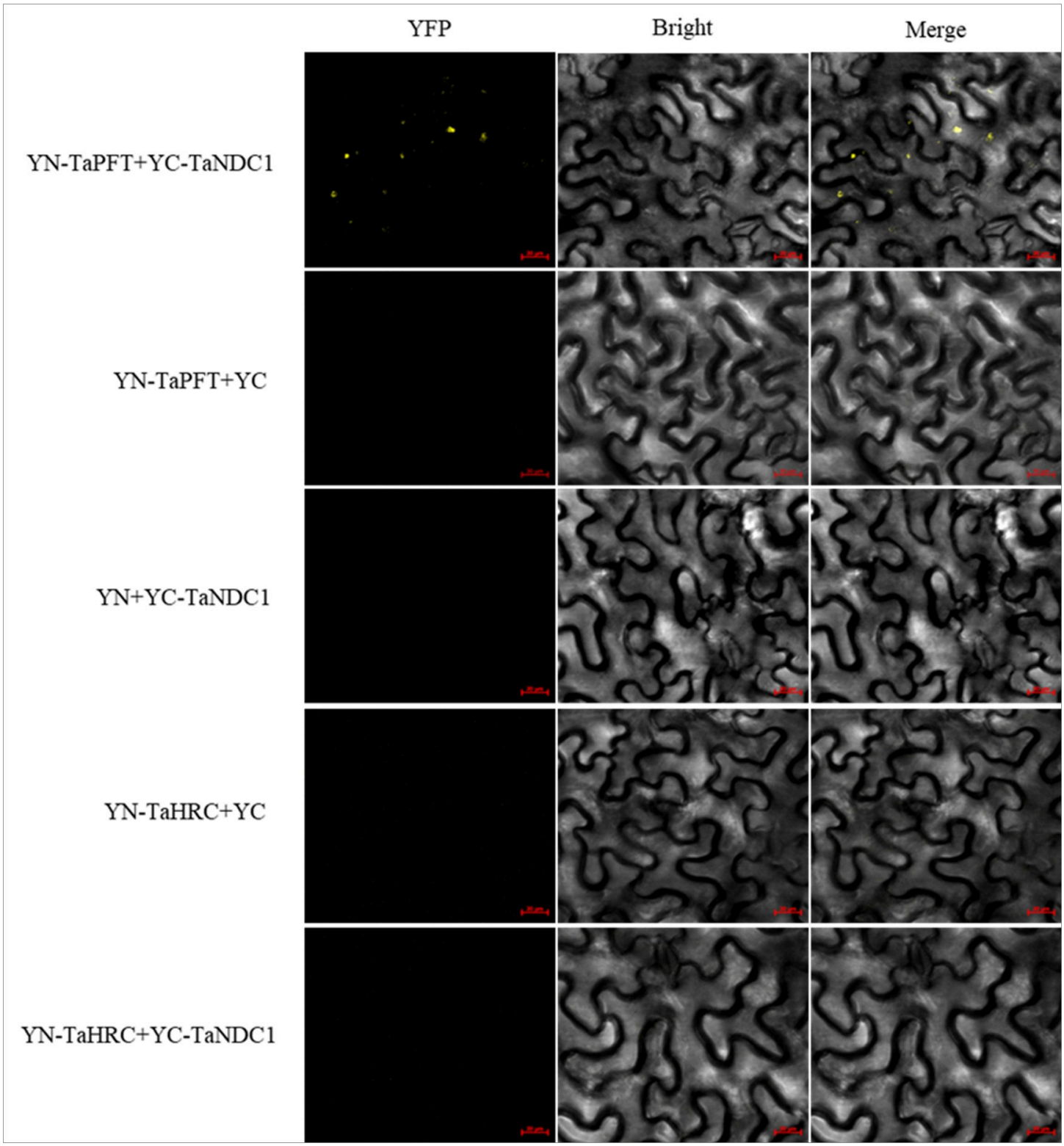


Figure 9

Bimolecular fluorescence complementation (BiFC) analysis of the interaction between TaNDC1 and TaPFT/TaHRC in N. benthamiana epidermal cells.

The experimental groups (YN-TaHRC + YC-TaNDC1,YN-TaPFT + YC-TaNDC1) and the negative controls (YN-TaPFT + YC, YN + YC-TaNDC1,YN-TaHRC + YC) were showed. Representative images from left to right show YFP fluorescence (YFP), bright-field view (Bright), and the merged channel (Merge).

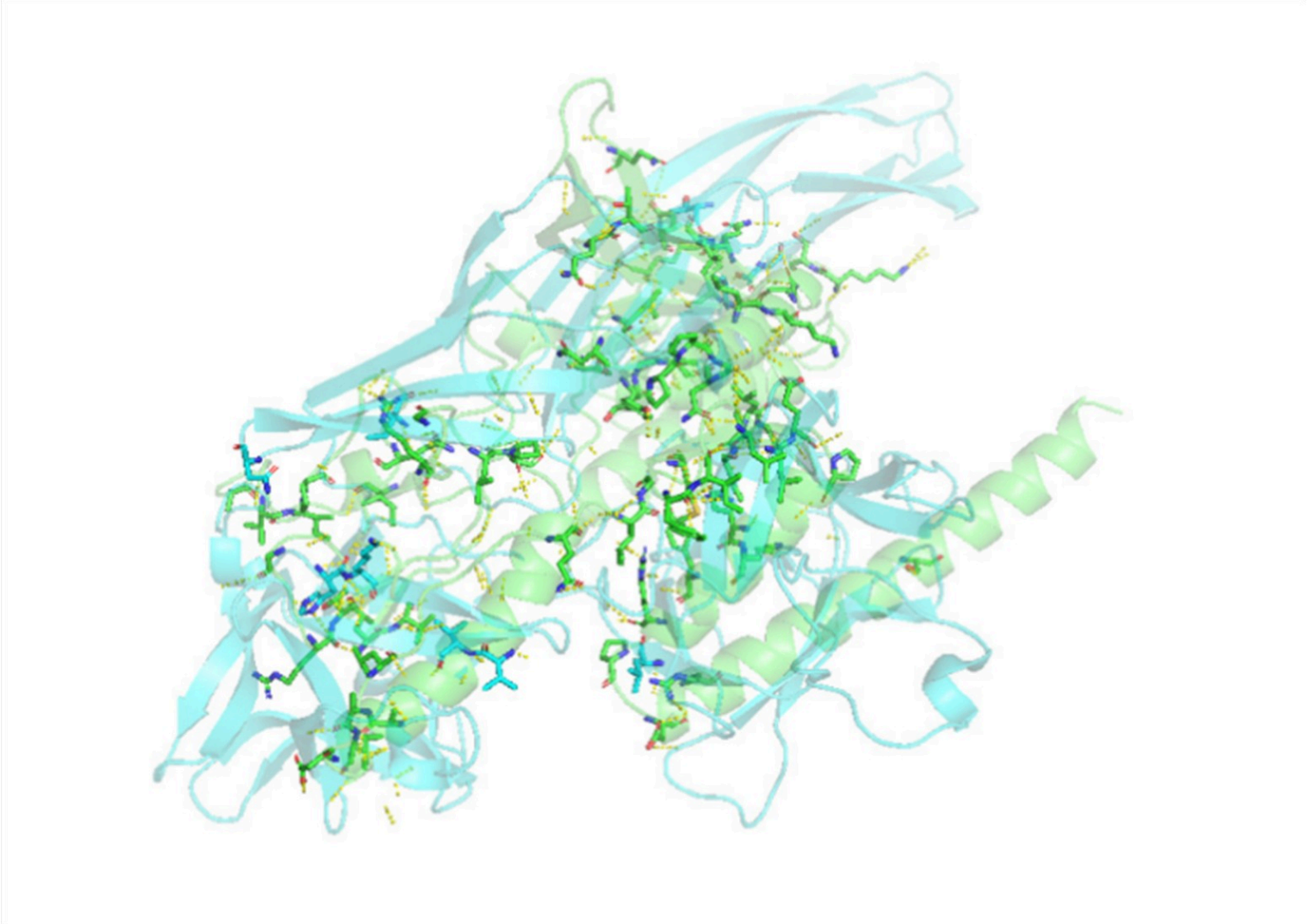


Figure 10

Molecular docking prediction of the interaction between TaNDC1 and TaPFT. Wheat TaPFT structure (blue color) is complexed with TaNDC1 structure (green color), highlighting catalytic (orange stick) and substrate-binding residues (red stick). The three-dimensional structural model was generated using AutoDock software and visualized with PyMOL, predicting a physical interaction interface between TaNDC1 and TaPFT.

Supplementary Files

This is a list of supplementary files associated with this preprint. Click to download.

- SupplementaryInformation.rar
- Tables.docx